SAND2017-6950J

A SOFTWARE FRAMEWORK FOR ASSESSING THE RESILIENCE OF DRINKING WATER SYSTEMS TO DISASTERS WITH AN EXAMPLE EARTHQUAKE CASE STUDY

Katherine A. Klise[1], Michael Bynum[2], Dylan Moriarty[1], and Regan Murray[3]

[1]Geotechnology and Engineering, Sandia National Laboratories, PO Box 5800, Mail Stop 0750, Albuquerque, NM 87185-1137, USA
[2]School of Chemical Engineering, Purdue University, 480 Stadium Mall Drive, West Lafayette, IN 47907, USA
[3]National Homeland Security Research Center, United States Environmental Protection Agency, 26 W. Martin Luther King Dr., Cincinnati, OH 45268, USA

Keywords
Water distribution system, earthquake, resilience, software

Abstract
Water utilities are vulnerable to a wide variety of human-caused and natural disasters. The Water Network Tool for Resilience (WNTR) is a new open source Python™ package designed to help water utilities investigate resilience of water distribution systems to hazards and evaluate resilience-enhancing actions. In this paper, the WNTR modeling framework is presented and a case study is described that uses WNTR to simulate the effects of an earthquake on a water distribution system. The case study illustrates that the severity of damage is not only a function of system integrity and earthquake magnitude, but also of the available resources and repair strategies used to return the system to normal operating conditions. While earthquakes are particularly concerning since buried water distribution pipelines are highly susceptible to damage, the software framework can be applied to other types of hazards, including power outages and contamination incidents.

1. Introduction
Depending on their location and vulnerability, drinking water utilities are taking steps to enhance their resilience to earthquakes, floods, drought, hurricanes, winter storms, forest fires, tornadoes, contamination incidents, terrorist attacks, and other types of hazards [1] [2] [3] [4] [5]. Resilience is defined by the National Academies of Science as “the ability to prepare and plan for, absorb, recover from, and successfully adapt to adverse events” [6]. The ability to maintain drinking water service during and following such hazardous incidents is critical to ensure the well-being and continuity of daily life. Water system resilience is important not only for individuals, but also for hospitals, schools, nursing homes, fire stations, restaurants, and for other industries that rely on water.

Natural disasters and other types of hazards have resulted in different types of water service disruptions: pipe breaks and leaks; power outages; failure of reservoirs, tanks, pumps, treatment plants, and other infrastructure; reduced water quality; loss of access to facilities and supplies; as well as financial, social, environmental and human health consequences [1] [7] [8]. Following large disruptive incidents like earthquakes, affected communities have experienced power outages and water service outages lasting from hours to weeks. For example, the 1994 magnitude 6.7 Northridge Earthquake, located outside Los Angeles, California, damaged seven reservoirs, over 60 transmission mains, and 1,000 distribution pipes. The quantity of water delivered was restored to pre-earthquake volumes after seven days, and the quality of water was restored and boil-water orders were lifted after 12 days. However, it took nine years to complete all repairs and restore full functionality of the water system [9]. Even though evidence shows that seismic-resistant pipes have a high survival rate following an earthquake [8], these upgrades have not been widely implemented because of the high cost for pipe replacement.

General guidance is available on water system resilience to disasters [1] [2] [3] [4] [5]; however, robust software tools to support utility-specific resilience assessment are not available. With such tools, water utilities could estimate potential damages to their system, understand the multitude of disruptions that could unfold over time, investigate redundancies, evaluate preparedness, and prioritize specific mitigation strategies, such as pipe replacement or adding redundancy to supply systems [2] [7]. Systems modeling tools have the potential to meet this need by combining disaster damage models with hydraulic and water quality models of water distribution systems. Additionally, systems modeling could incorporate changes in customer behavior during disasters (e.g., water usage), as well as utility response actions. This type of simulation approach could allow a water utility to design more effective mitigation activities before a disaster occurs.

This paper presents a comprehensive software framework for assessing the resilience of drinking water systems to disasters, including earthquakes. The software improves upon currently available capabilities by fully integrating hydraulic and water quality simulation, damage estimates and response actions, and resilience metrics into a single platform. This software is available as an open source software package called the Water Network Tool for Resilience (WNTR, pronounced *winter*). In the rest of this paper, the relevant literature is reviewed, the WNTR software framework is described in detail and then an earthquake case study is presented to demonstrate the capabilities in WNTR. While the case study focuses on earthquakes, the software framework is general and can be applied to a wide range of disruptive incidents and repair strategies.

2 Literature Review

Existing hydraulic and water quality modeling software tools were not designed to handle sudden failures resulting in inadequate pressure or rapid changes in system operation. Moreover, they were not designed to handle situations when sections of a water system become isolated, tanks or reservoirs drain, or the system operational rules cannot be met. For example, commonly used demand-driven (DD) hydraulic simulators, like EPANET [10], assume customer demands are always met even if the pressure is insufficient to provide the demand. In reality, disasters can lead to situations where pressure in the system is unusually low and customer demand would not be met.

Several alternatives to DD simulators have been discussed in the literature. Wagner et al. [11] presented pressure-driven demand (PDD) hydraulic equations for water distribution systems in which the demand supplied to a node is a function of the pressure at that node [12]. During low-pressure conditions, customers receive a fraction of their expected demand. PDD simulators include WaterNetGen [12] [13], which is an open source software tool, and WaterGEMS™ [14], which is a commercial software tool. Quasi-PDD simulators (or semi-PDD) run DD simulations in an iterative manner and nodes are switched between constant-demand nodes, zero-demand nodes, and (sometimes) emitters depending on the domain in which the pressure falls [15] [16] [17]. When considering disaster scenarios, the difference between using DD and PDD simulation can be drastic [18].

After a large-scale disruption, water demand in the network can change dramatically. Structural damage and emergency operational changes can result in isolated sections of the network or low pressure conditions that reduce the amount of water delivered to customers. Policy changes, including do-not-drink orders, boil-water orders, or water conservation efforts, also decrease customer demand. When planning for an adequate drinking water supply during emergencies, water utilities need to account for the minimum acceptable water use per capita, the anticipated time scale of the disruption, the population impacted, and water quality standards that need to be upheld [19]. If acceptable water volume and quality cannot be delivered, potable water alternatives would have to be considered. Customer behavior can also change during emergencies, either temporarily increasing demand (e.g., filling up bathtubs to stockpile water) or decreasing demand (e.g., relying on bottled water because of a lack of confidence in the delivered water). These changes in customer demand can impact resilience; for example, conservation might increase water availability for firefighting.

Several tools have been developed to estimate the hydraulic performance of a water distribution system after an earthquake [17] [20] [21] [22]. These tools use attenuation models and fragility curves developed by the American Lifeline Alliance to estimate network damage based on earthquake magnitude and location [23] [24] [25]. Attenuation models calculate peak ground acceleration (PGA) and peak ground velocity (PGV) as a function of earthquake magnitude, location and depth. Fragility curves determine the probability of damage as a function of ground movement. These models are generally built on empirical data from recent earthquakes, which includes information such as the characteristics of damaged pipes and the measured PGA. The Graphical Interactive Serviceability Analysis of Life-Lines subjected to Earthquakes (GISALLE) tool quantifies water service availability after an earthquake and uses the Loma Prieta Earthquake as the basis for a stochastic parametric study [22]. The Graphical Iterative Response Analysis for Flow Following Earthquakes (GIRAFFE) software builds upon GISALLE to include upgrades to the way low pressure conditions are handled when modeling pipe failure and includes a seismic wave model to estimate joint damage [21]. Mani et al. [20] include pipe leak models developed by Shi et al. [21] and use the Tehran water distribution network as a case study. The Reliability EVAluation model for Seismic hazard for water supply NETwork (REVAS.NET) tool includes earthquake attenuation models and probabilistic scenarios with different repair strategies [17]. Guidotti et al. [26] extend previous work by including a general procedure for modeling resilience of critical network infrastructure. This work includes methods that account for dependencies between networks, such as the water distribution systems and the electric power network. The general procedure can be applied to a wide range of hazards and recovery actions. To date, these research efforts use quasi-PDD hydraulic simulations.

Several studies have simulated the damage to the Los Angeles Department of Water and Power caused by the 1994 Northridge Earthquake in California and the restoration activities that followed [27] [28] [21]. These tools combine GIRAFFE with the capability to demonstrate restoration actions, such as sending crews to investigate, isolate, and repair pipe breaks. Other modeling tools were developed to help the East Bay Municipal Water District in Northern California manage earthquake response in real-time, prioritize transmission line upgrades, and assess interdependencies with the electricity sector [29]. These tools combine real-time USGS ShakeMap data on ground movement after an earthquake [30] with a customized software tool to rapidly predict damage to specific water utility assets [29].

3. Modeling Framework

The United States Environmental Protection Agency, in partnership with Sandia National Laboratories, developed WNTR to integrate critical aspects of resilience modeling for water distribution systems into a single software framework. WNTR provides a flexible platform for modeling both disruptive incidents and repair strategies in water distribution systems. WNTR advances previous research by making major improvements to hydraulic simulations including PDD, the ability to add and repair leaks, and the ability to change operations and/or response strategies in the middle of a simulation. Additionally, WNTR combines damage and response models into a single framework, allowing for a seamless evaluation of response and/or mitigation strategies to minimize overall consequences to the water utility. The primary modeling components in WNTR include: (1) disaster models (e.g., attenuation models to predict ground movement after an earthquake), (2) fragility curves used to assign the probability of damage to network components, (3) flexible controls to change the status and operation of network components, (4) models to estimate leaks in the network, (5) PDD hydraulic simulation to model the network during low pressure conditions, (6) resilience metrics to evaluate the effect of the disruption and repair strategies, and (7) the ability to perform Monte Carlo simulations.

WNTR is a Python package, which requires Python (2.7, 3.4, or 3.5) along with several Python package dependencies, including NetworkX, Pandas, Matplotlib, NumPy, and SciPy. A water network model can be constructed within WNTR or created from an EPANET formatted water network model input file. Connectivity of the water network (i.e., the network layout) is stored as a NetworkX data object [31]. The NetworkX package facilitates use of numerous methods to analyze the structure of complex networks. Results from hydraulic and water quality simulations are stored as Pandas data objects [32], which allows for powerful time series analysis of node and link attributes, such as pressure and flow. WNTR includes high-quality graphics capabilities, including network graphics and animation, using Matplotlib [33]. A dependence on NumPy and SciPy [34] enables efficient numerical computation, and working within the Python environment facilitates simulations run in loops or in parallel using standard Python methods [35]. In addition to the features listed above, WNTR is compatible with all unit conventions of EPANET formatted water network model input files.

WNTR integrates these components into a single easy-to-use software platform for evaluating resilience of water distribution systems. Leveraging the object-oriented programming capabilities of Python, WNTR easily performs many complex analyses. Note that the object-oriented EPANET Python package, OOPNET, makes use of similar Python packages to facilitate scientific computing but currently only uses EPANET for hydraulic simulations, limiting the tool to DD hydraulic simulations [36]. WNTR can perform DD simulations using EPANET or PDD simulations using WNTR's own hydraulic solver. The program interface is flexible and allows users to make changes to the network structure and operations, and add disruptive events and recovery actions.

3.1 Software Availability

WNTR can be installed through the U.S. Environmental Protection Agency GitHub organization at https://github.com/USEPA/WNTR. The software was made publically available in October 2016. The GitHub site includes links to software documentation, software testing results, and contact information. The software documentation includes Python code to demonstrate the application program interface (API) and code structure. Python distributions, such as Anaconda, are recommended to help users manage the Python environment.

3.2 Earthquake Attenuation Models

WNTR includes attenuation models that describe how seismic waves diminish as they travel away from the epicenter. The energy associated with a seismic wave is commonly measured in terms of PGA and PGV. Attenuation models are often developed using data from a particular earthquake and depend on the local geology. Many models exist and choosing an appropriate model for a particular study area can be difficult. Infrastructure damage is associated with both PGA and PGV. Pump and tank damage is often estimated using PGA, whereas PGV is frequently used to estimate repair rate for pipes. Repair rate is defined as the number of repairs needed per km of pipe. Correction factors can be applied to the repair rate to account for variation in pipe material and soil type. The PGA attenuation models in WNTR include:

$$PGA = 403.8 \times 10^{0.265M}(R+30)^{-1.218} \tag{1}$$
$$\ln(PGA) = 0.4 + 1.2M - 0.76\ln(D) + 0.0094D \tag{2}$$
$$\log(PGA) = -1.83 + 0.386M - \log(R) - 0.0015R \tag{3}$$

where M is the earthquake magnitude (unitless), R is the distance to the epicenter (km), and D is the distance to the focus (km) [37] [38] [39]. These are the same PGA models used in REVAS.NET. The PGV attenuation models in WNTR include:

$$PGV = 10^{0.848+0.775M+1.834(R+17)} \tag{4}$$
$$PGV = 10^{-0.285+0.711M-1.85(R+17)} \tag{5}$$

where Eq 4 is for rock and Eq 5 is for soil [40]. Since attenuation models are commonly developed for a particular earthquake and site, analysts often use the average of several models to capture general trends [17] [23]. PGV is used to compute a pipe repair rate. The following linear and power law repair rate (RR) models from [23] are included in WNTR:

$$RR = 0.00187 \times PGV \quad (6)$$
$$RR = 0.00108 \times PGV^{1.173} \quad (7)$$

To include pipe and soil characteristics in the calculation, RR is multiplied by a correction factor [41], which is a function of pipe diameter, pipe material, topography, and liquefaction potential. A weight is assigned to different categories. Correction factor (C) is computed as follows:

$$C = C_d \times C_m \times C_t \times C_l \quad (8)$$

where C_d is the correction factor for pipe diameter (unitless), C_m is the correction factor for pipe material (unitless), C_t is the correction factor for topography (unitless), and C_l is the correction factor for liquefaction potential (unitless). By default, WNTR uses the categories and weights supplied in [41] but users can customize categories and weights by modifying input to the code. Additional models for PGA, PGV, RR, and C can be added by the user or included in a future release of the software. Users can also import data from external sources, such as USGS ShakeMap.

3.3 Fragility Curves

Fragility curves define the probability of exceeding a damage state as a function of environmental change. Fragility curves are commonly used to predict network damage after an earthquake caused by ground motion. Fragility curves are closely related to survival curves, which are used to define the probability of component failure due to age. Network components can have multiple damage states, for example, a pipe can be subject to major or minor leaks. To estimate damage caused by an earthquake, fragility curves are defined as a function of PGA, PGV, or RR. The American Lifelines Alliance reports [23] [24] include seismic fragility curves for water system components. Damage to above ground pumps, tanks, and tunnels is often estimated using PGA, while damage to below ground pipes is often estimated using PGV and RR [23] [24]. WNTR includes methods to define fragility curves (or survival curves) with multiple damage states using a wide array of statistical distributions. The fragility curves are then used to assign a probability of damage for each network component. The damage state is determined stochastically by selecting a uniform random variable for each network component and the water network model is adjusted accordingly to reflect the damage state that is selected. Fragility curves can also be used to estimate damage from other types of disasters, for example, fragility curves can be defined as a function of flood stage, wind speed, or temperature. FEMA's HAZUS software can also be used to estimate damage to water distribution systems from earthquakes and floods [42] [43]. The output from HAZUS can be used in WNTR to adjust model components and reflect damage states.

3.4 Flexible Controls

Similar to EPANET, network controls in WNTR include time-based and conditional rules that govern how the network is operated. In EPANET, these controls can be used to change link status (open, closed, or active) or settings (pump speed or control valve setting). WNTR extends the controls available in EPANET to include a wide range of component status and settings. For example, conditional controls can be defined to simulate cascading failures where pipe leaks start when pressures exceed a critical threshold. Time-based and conditional controls can also be used to start and stop leaks and power outages or to stop the hydraulic simulation. Hydraulic simulations can also be paused while controls are changed and the simulation can then be restarted.

3.5 Leak Model

Leaks can cause large changes in network hydraulics. WNTR can be used to explicitly model water lost due to a leak between the time when it starts and the time when repair crews can isolate the leak by using available valves. WNTR can simulate leaks at junctions and tanks or at any location along a pipe by splitting the pipe into two sections and adding a junction connecting the two new pipe sections. Pipe breaks can be modeled by removing the existing pipe, adding two new junctions with leaks, and adding two new pipes connecting the new junctions to the network. In this case, the two new junctions are not connected to each other (preventing flow between the two junctions that were connected by the original pipe). In WNTR, leaks are modeled with a general form of the equation proposed by Crowl and Louvar [44] where the mass flow rate of fluid through the hole, d^{leak}, is expressed as:

$$d^{\text{leak}} = C_d A \sqrt{2\rho} p^{\alpha} \tag{9}$$

where C_d is the discharge coefficient (unitless), A is area of the hole (m^2), ρ is the density of the fluid (kg/m^3), and p is the gauge pressure inside the pipe (Pa). The default discharge coefficient is 0.75 (assuming turbulent flow [45]), but the user may specify other values if needed. The value of α is set to 0.5 (assuming large leaks out of steel pipes [45]). As described by Lambert [45], the primary factors affecting C_d and α are flow regime, pipe material, and orifice shape (longitudinal, round, circumferential). Additionally, both C_d and A may vary with pressure. Future development of WNTR will include extension of Eq. (9) to account for these factors. For example, a linear model may be used to describe the area as a function of pressure as in [46].

3.6 Pressure-Driven Demand Hydraulics

WNTR uses a PDD model proposed by Wagner et al. [11] :

$$d = \begin{cases} 0 & p \le P_0 \\ D_f \sqrt{\frac{p - P_0}{P_f - P_0}} & P_0 < p < P_f \\ D_f & p \ge P_f \end{cases} \tag{10}$$

where d is the actual demand delivered to customers (m^3/s), D_f is the customers expected demand (m^3/s), p is the pressure (Pa), P_f is the pressure above which the customer should receive the expected demand (Pa), and P_0 is the pressure below which the customers cannot receive any water (Pa). P_f and P_0 can be defined at each node and can be modified by the user. The set of nonlinear equations describing network pressures and flows comprising the hydraulic model, including (10), is solved directly using a Newton-Raphson algorithm. However, Newton-Raphson algorithms do not guarantee convergence if the derivatives of the equations of interest are not Lipschitz continuous [47]. The derivative of the PDD equation above is not Lipschitz continuous or even continuous; therefore, a cubic Hermite spline is applied when p is near P_0 and P_f to enforce continuity.

3.7 Resilience Metrics

Resilience is the ability of a system to minimize disruption and return to normal function after a disaster. Metrics that quantify resilience need to account for system function before, during, and after the disruption. Numerous resilience metrics have been suggested [7], including metrics that compute redundancy, robustness, reliability, rapidity, adaptability, and resourcefulness. For water distribution systems, these metrics generally fall into four categories: topographic, hydraulic, water quality/security, and economic. While some metrics define resilience as a single quantity, other metrics are a function of time, space, or both. For this reason, state transition plots [48], network graphics, and network animation are useful ways to visualize resilience metrics. When quantifying resilience, it is important to understand which metric best defines resilience for a particular disaster or response scenario. For example, topographic metrics are useful when studying the effect of adding redundant pipes while hydraulic metrics are useful when studying the effect of pipe breaks. Numerous resilience metrics can be computed using WNTR. These metrics include shortest path lengths [31], articulation points [31], Todini resilience index [49], and water service availability [9], among others. Some metrics can also be converted to capture statistics about the population served. For example, WNTR can be used to compute the number of people that are impacted by water service availability less than a critical threshold.

The metrics used in the case study below include water service availability and population impacted. Water service availability is computed as follows:

$$WSA_t = (\sum_{n \in N} V_{nt}) / \left(\sum_{n \in N} \hat{V}_{nt}\right) \quad (11)$$

where WSA_t is the water service availability of the network (unitless) at time t, N is the set of network nodes, V_{nt} is the actual water volume received (m^3) at node n at time t, $\hat{V}_{nt}$ is the expected water volume (m^3) received at node n at time t. Resilience metrics, like WSA, that depend on expected water demand can be influenced by changes in customer behavior after a disaster. Water conservation efforts, for example, change the expected demand of customers. It is important to model expected customer behavior after disasters to account for the impact this might have on resilience.

Population at each node is computed as follows:

$$pop_n = \frac{q_n}{R} \quad (12)$$

where pop_n is the population at node n, q_n is the average water volume consumed per day (m^3/day) at node n under normal conditions, R is the average volume of water consumed per capita per day (m^3/day). For this study, R is set to 0.76 m^3/day (200 gallons/day). This calculation does not account for population movement throughout the day.

The population at a given node is "impacted" by the disruption if they receive less than a fixed percentage of their expected water volume. Population impacted is computed as follows:

$$PI_t = \sum_{n \in N} pop_n \delta_{nt} \text{ where } \delta_{nt} = \begin{cases} 1 \text{ if } V_{nt}/\hat{V}_{nt} < \tau \\ 0 \text{ otherwise} \end{cases} \quad (13)$$

where PI_t is the population impacted at time t, d_{nt} is a binary variable that is set to 1 if $V_{nt}/\hat{V}_{nt}$ is less than a threshold, τ, and set to zero otherwise. The threshold is set to 80% in the case study below.

3.8 Monte Carlo Simulation

To address the uncertainty associated with modeling potential disasters, Monte Carlo techniques can be used to simulate multiple realizations or outcomes of a given scenario. WNTR has the capability to allow characteristics of a disaster scenario to be drawn from statistical distributions. As mentioned above, fragility curves provide probabilities of the location and severity of a disruption. The duration of the disruption can also be drawn from statistical distributions. Distributions can be a function of component properties (e.g., pipe age, material, or joint type), environmental change (e.g., PGA, PVG, or RR), or available resources (e.g., number of repair crews available). WNTR is compatible with many statistical distributions and random selection methods that can be used for stochastic simulation. WNTR also includes the ability to pause the hydraulic simulation, change network operations, and then restart the simulation. The water network model and simulation results can also be saved to files and reloaded for future analysis. These features are helpful when evaluating various response action plans and when simulating long periods with different time resolution. Standard Python tools can also be used to run simulations in parallel [35].

4. Earthquake Case Study

The following case study demonstrates multiple capabilities of WNTR that can be used to evaluate disruptive incidents and repair strategies after an earthquake. Figure 1 shows the network model of a real water distribution system that is used for the case study [50]. The system serves approximately 152,000 customers and has one reservoir, two valves, 34 tanks, 61 pumps, 3,323 nodes, and 3,829 pipes. The pipes are made of cast iron, ductile case iron, and polyethylene and the soil type in the region has various degrees of liquefaction potential (Figure 1). The spatial distribution of these properties was used to determine pipe fragility, as described below.

An earthquake was assumed to have occurred at 6:00 AM along an N-S fault that parallels a valley on the west side of the network (Figure 2). In the model, this was 24 hours after the start of the simulation. The earthquake epicenter was assumed to have occurred at the south, central, or north part of the city, with a magnitudes of 6.0, 6.5, or 7.0. The hydraulic response of the network was simulated for 14 days after the earthquake. PDD hydraulic simulations were run using a minimum and nominal pressure of zero and 25 psi, respectively. In the simulations, ground movement from the earthquake damaged pipes and tanks, pumps stopped operating due to either direct damage or power outages, and damaged natural gas pipelines cause fires. Given the disorder that ensues after an earthquake, especially after large earthquakes, it was assumed that repairing network components and fighting fires was not possible for the first 12 hours after the earthquake occurs (note that 12 hours might be too long in some cases and this value can be adjusted). After that period, fire crews were scheduled to fight fires and repair crews were scheduled to fix damaged components in the network. Three repair strategies including water conservation and seismic-resistant pipes were simulated. Network resilience was quantified using two metrics, water service availability and population impacted, computed using Eq. 11 and 13, respectively. To incorporate uncertainty in outcomes, 50 realizations of each of the 27 scenarios were run (three earthquake locations, three earthquake magnitudes, and three repair strategies).

4.1. Earthquake damage

For this case study, network component damage includes tank and pipe leaks, and pump failure. For each tank, pump, and pipe, fragility curves were used to define the probability of damage as shown in Figure 3. For tanks, the fragility curves in Figure 3A included four damage states (DS): DS1 resulted in a leak with diameter 0.05 m, 0.25 m for DS2, 0.5 m for DS3, and 1 m for DS4. For pumps, there was a single damage state, DS1, associated with pump shut off (Figure 3B). For pipes, there were two damage states: DS1 resulted in a minor leak for which the leak diameter was drawn from a uniform distribution with a minimum of 0.01 m and a maximum of 0.05 m, while DS2 represented a major leak with a diameter from 0.05 m to 0.15 m (Figure 3C). Leaks were added to the midpoint of the pipe, and were constrained to not to exceed 75% of the pipe diameter.

For each scenario and realization, PGA, PGV, and RR was computed for each network component. Here, PGA was computed using the average of Eq. 1, 2 and 3. As an example, Figure 4A shows the spatial distribution of PGA for a magnitude 6.5 earthquake at the central location. PGV was computed using the average of Eq. 4 and 5. RR was computed using Eq. 6 from PGV and a correction factor that was computed using Eq. 8 with the default weights defined in [41].

The damage state for each component was then determined stochastically based on the PGA or RR calculated for the component and a uniform random variable selected for that component. The fragility curve incorporates both of these values: PGA or RR determines the x-axis value while the random variable determines the y-axis value. The intersection point of these values determines the damage state for a particular component for a single realization. The water network model was then adjusted to reflect the selected damage: if a pump was damaged, a control was added that changed its status to off; new nodes were added to the network model to represent leaks. As an example, the location of pipe and tank damage resulting from a magnitude 6.5 earthquake at the central location is shown in Figure 4B.

While damage to other network components such as reservoirs, turbines, and treatment plants were not included in this study, similar methods could be used to define the probability of damage to these components and the network could be modified accordingly.

Fires are important to include when modeling the effects of an earthquake because water utilities are responsible for maintaining enough capacity to fight fires. For this case study, the locations of fires were randomly distributed throughout the network. Typical firefighting demands and durations [51] were added to the network model to simulate the water withdrawal needed to fight one fire every 12 hours over the full duration of the simulation. For each fire, demand was selected from a uniform distribution with a minimum of 1500 gallons/min and a maximum of 8000 gallons/min. Duration was selected from a uniform distribution with a minimum of two hours and a maximum of four hours.

4.2. Repair strategies

Three repair strategies were considered in this case study. For all strategies, repairs began 12 hours after the earthquake. There were five repair crews to fix pipe damage, two repair crews to fix tank damage, one repair crew to fix pump damage, and one firefighting crew. In the first repair strategy (RS1), customer expected demand continued at their normal rate after the earthquake. In the second repair strategy (RS2), customer expected demand was reduced by 40% for 14 days after the earthquake. This was done to simulate the impact of water conservation after the disaster. In the third strategy (RS3), the utility retrofitted pipes near the fault zone to be seismic-resistant and customer expected demand continued at their normal rate after the earthquake. In this case, pipes in the 'partial liquefaction' zone (Figure 1), did not sustain damage after the earthquake.

The pipe and tank repair crews fixed one leak every 12 hours. Within the first six hours, the leaks were isolated using valves at the nearest junctions, and the leak was fixed within the next six hours. After the leak was repaired, the pipe was opened. To stagger repairs, the exact time of isolation and repair were drawn from a uniform distribution within the first or second six-hour period. Repairs were prioritized based on the largest cumulative leak volume at the time of each repair. As leak rates can increase or decrease through time as the pressure fluctuates, this prioritization changed throughout the simulation. Within WNTR, the simulation was paused every 12 hours, the cumulative leak rates were computed, and the largest five pipe leaks and largest two tank leaks were scheduled for repair.

The single pump repair crew fixed one pump every eight hours. In this network, the reservoir is near the lowest point in the network, and pumps are critical to deliver water to customers in the upper sections of the network. For this reason, pump repairs were prioritized based on pipe distance to the reservoir, with the closest pump fixed first. Since this prioritization does not include feedback from the simulation, the simulation does not have to be paused to schedule pump repairs.

For this case study, there was one fire crew to fight a fire every 12 hours, and the fires were fought in a random order. If the pressure was not sufficient to pull the required water volume, the hydraulic simulation continued to try to extract the expected demand for the duration of the fire. The difference between the expected and actual demand was recorded for each fire to measure water service availability for firefighting.

The earthquake damage and repair strategies used in this case study were based on reasonable assumptions. These parameters can all be adjusted within WNTR to customize analysis for a specific water utility and disaster scenario.

4.3 Case study results

Figure 5 shows the results of a single realization of a magnitude 6.5 earthquake at the central location with RS1. For this realization, 239 pipes were damaged, 7 tanks were damaged, and 14 pumps lost power. Figure 5 shows the leak rates on all 239 damaged pipes and the tank levels for all 34 tanks as a function of time. As Figure 5A shows, the leak rates were high until the pipes were repaired. However, as the network was repaired and pressures increased, new leaks were sometimes discovered and subsequently repaired, as shown with the leak highlighted in red in Figure 5A. That particular leak was fixed 9.1 days after the earthquake. Figure 5B shows how tank levels (from both damaged and non-damaged tanks) varied as components were repaired. In that figure, tank levels from damaged tanks are highlighted in red. Once the tank was repaired, the tank level is shown in gray. Figure 5B also shows that some tanks that were not damaged by the earthquake can drain due to damage at other locations in the network.

Figure 6, Figure 7, and Figure 8A show the results for 50 realizations of the same earthquake magnitude (6.5), location (central), and repair strategy (RS1). For each realization, different network components were damaged as defined by the probability distribution functions in the fragility curves and by different fire demands assigned to different locations. Similarly, pipes and tanks were repaired in a different order according to the prioritization for leak repair and fires were fought in a random order. Figure 6 shows the water service availability of the network over time, reflecting the proportion of customer expected demand that was actually delivered for the entire network. As the customer expected demand vary on a diurnal cycle, so does the water service availability. A day after the earthquake, water service availability varied from about 45% to more than 60%, showing the potential range in outcomes for the same scenario. The median value (in black) reached a low of 54% and slowly returned to full service at 6.58 days after the earthquake. The median value was used here to compute a recovery time, defined as the time when the system could deliver 90% of the pre-earthquake water volume to customers.

Figure 7 shows the firefighting capacity for the same 50 realizations. Firefighting capacity is defined as the water service availability at the nodes where fire demand was added to the system. The quantity is computed at the same frequency as the fires occur, which is 12 hours in this case. The results show that firefighting capacity varies widely and slowly recovered over the 14 day simulation. After one day, firefighting capacity varied from about 15%-85% for the 25th to 75th percentile scenarios, but ranged from about 75%-100% by the end of the 14 days.

Figure 8 shows the population impacted for each of the 50 realizations. With no conservation efforts (RS1) between 70,000 and 100,000 people were impacted a day after the earthquake, receiving less than 80% of their expected water volume. Based on the median value of the 50 realizations, almost 90,000 people were impacted. The recovery time was defined as the time when less than 10% of the population was impacted. For RS1, it took 7.08 days to meet this level. Figure 8B shows the same results when water conservation efforts were in place (RS2) immediately following the earthquake. This shows that the population impacted was much lower with conservation strategies in place. Based on the median value, approximatly 53,000 people were impacted, and the time to recovery was reduced to 4.04 days. Figure 8C shows results when pipes were retrofitted to be seismic-resistant near the fault line. These results show dramatic reduction in the number of people impacted and the time to recovery, median result indicate that less than 26,000 people were impacted and the time to recovery was just 1.58 days after the earthquake.

Table 1 and Table 2 summarize the minimum water service availability, maximum population impacted, and time to recovery for each magnitude, location, and repair strategy. These values were computed using the median value for each scenario over all 50 realizations. As expected, water service availability decreased and population impacted increased as the earthquake magnitude increases. Unsurprisingly, the location of the earthquake also had an impact on water service availability and population impacted. Earthquakes at the northern location, further from the city, had less of an impact than earthquakes occurring in the city. Given RS1 conditions, earthquakes of magnitudes 6.5 or greater at the south and central locations impacted the network almost equally. To further illustrate this point, Figure 9 shows the distribution of maximum population impacted over all 50 realizations when the earthquake was located at the north, central, and southern epicenter and RS1 is used. This comparison shows that while location can have a large influence on population impacted, the results can vary widely depending on the specific network damage and response strategy. Table 1 and Table 2 also illustrate that both water conservation and earthquake resistant pipes in the liquefaction area helped to increase overall water service availability and decrease population impacted. Under most scenarios the use of earthquake resistant pipes was slightly more effective than water conservation, however, earthquake resistant pipes were significantly better for earthquakes occurring the central location near the retrofitted pipes.

Overall, these results indicate that this network could expect to withstand a magnitude 6.0 earthquake with only 2-15% reduction in water service availability, and less than 34,000 customers impacted. In contrast, a magnitude 7.0 earthquake could be expected to affect more than 85% of customers, result in a minimum water service availability of 0.27-0.35, and require more than 14 days to recover. This case study is intended to illustrate how water utilities could use WNTR to evaluate disruption and resilience-enhancing actions following an earthquake. Similar analysis could be used to evaluate other types of disruptions and utility specific data could be used to validate the model.

5. Summary and Conclusions

Drinking water systems are subject to a wide range of hazardous incidents that can disrupt service to customers and damage critical infrastructure. This paper introduces WNTR, a new open source Python package designed to help water utilities investigate resilience of water distribution systems to a wide range of hazardous scenarios and to evaluate resilience-enhancing actions. Unlike current modeling tools, WNTR integrates hydraulic and water quality simulation, a wide range of damage and response options, and resilience metrics into a single framework, allowing for a seamless evaluation of water network resilience. The software can help water utilities estimate potential damages, understand how damage to infrastructure would occur over time, evaluate preparedness strategies, prioritize response actions, and identify worse case scenarios, efficient repair strategies, and best practices for maintenance and operations.

While a few modeling tools have been developed that focus on evaluating the resilience of water networks after an earthquake, WNTR was designed to simulate a wide range of disaster scenarios, including earthquakes, contamination incidents, and power outages. The software includes methods to predict infrastructure damage using fragility or survival functions, and other approaches can be added using the flexible Python environment. WNTR allows the user to change features of the network model to reflect damage, and initiates leaks in pipes or tanks as necessary. By simulating hydraulics using PDD the effects of pipe breaks or damaged tanks on system pressures and delivered water volumes is more accurately predicted. Moreover, WNTR allows for simulation to continue even when parts of the water system are isolated and unable to provide water to customers. In this way, WNTR is able to estimate the performance of a drinking water system during extreme failures which is a significant advancement from current modeling tools. WNTR also provides more flexibility by allowing the user to change system controls and model components mid-simulation.

In this paper, several response strategies were demonstrated including fixing pipe leaks, repairing tanks, restoring power to pumps, fighting fires, and implementing conservation strategies. WNTR can also be used to simulate the response to contamination events by, for example, flushing contaminated water from hydrants or instituting do-not-drink orders. Mitigation strategies, such as installing online monitoring early warning systems, can also be modeled within WNTR. Optimization of response and mitigation strategies is an area of ongoing research that could be added to WNTR in the future.

WNTR contains a wide variety of metrics that can serve as indicators of resilience, including topographic, hydraulic, and water quality measures, some of which are measured at the node or pipe level and some at the system-level. For this paper, two metrics were used: water service availability and population impacted. These are system-level metrics reflecting the ability of the entire water system to withstand and recover from disasters. These types of metrics can be used to compare a water system's resilience across different types of disasters, and to measure improvements in resilience based upon newly implemented mitigation actions or planned response strategies. In this context, it is important to consider how different system functions recover (i.e. firefighting capacity, water availability, water quality) when customers are asked to conserve resources. Further research is needed to assess the most useful resilience metrics for water systems and to fully understand how systems-level metrics embody resilience characteristics.

Future development will focus on modeling critical interdependencies with other infrastructure sectors, such as the electrical sector, simulation and analysis of additional disaster scenarios based on real events, optimization of response actions, and network design or retrofit strategies that improve resilience. In addition, the effect of customer behavior after a disruption (e.g., evacuation, water conservation, disruption to work schedules) will be further studied and incorporated into WNTR.

Acknowledgement
The U.S. Environmental Protection Agency (EPA) through its Office of Research and Development funded and collaborated in the research described here under an Interagency Agreement with the Department of Energy's Sandia National Laboratories. It has been subjected to the Agency's review and has been approved for publication. Note that approval does not signify that the contents necessarily reflect the views of the Agency. Mention of trade names products, or services does not convey official EPA approval, endorsement, or recommendation. Sandia National Laboratories is a multimission laboratory managed and operated by National Technology and Engineering Solutions of Sandia, LLC., a wholly owned subsidiary of Honeywell International, Inc., for the U.S. Department of Energy's National Nuclear Security Administration under contract DE-NA0003525.

References

[1] Critical Infrastructure Partnership Advisory Council (CIPAC), "All-Hazard Consequence Management Planning for the Water Sector: Preparedness, Emergency Response, and Recovery CIPAC Workshop," US Department of Homeland Security, Washington DC, 2009.

[2] American National Standards Institute (ANSI), "Risk Analysis and Management for Critical Asset Protection (RAMCAP®) Standard for Risk and Resilience Management of Water and Wastewater Systems," American Water Works Association, Denver, CO, 2010.

[3] US Environmental Protection Agency (USEPA), "Flood Resilience: A Basic Guide for Water and Wastewater Utilities," US Environmental Protection Agency, Office of Water, EPA 817/B-14/006, Washington DC, 2014.

[4] US Environmental Protection Agency (USEPA), " Power Resilience Guide for Water and Wastewater Utilities," US Environmental Protection Agency, Office of Water, EPA 600/R–15/004, Washington DC, 2015.

[5] US Environmental Protection Agency (USEPA), "Drought Response and Recovery: A Basic Guide for Water Utilities," US Environmental Protection Agency, Office of Water, EPA 810/B-16/001., Washington DC, 2016.

[6] National Academy of Sciences (NAS), "Disaster Resilience: A National Imperative," prepared by the NAS Committee on Science, Engineering, and Public Policy. The National Academies Press, Washington, DC, 2012.

[7] US Environmental Protection Agency (USEPA), "Systems Measures of Water Distribution System Resilience," US Environmental Protection Agency, Office of Research and Development, EPA 600/R–14/383, Washington DC, 2015.

[8] J. Eldinger and C. A. Davis, "Recent Earthquakes: Implications for U.S. Water Utilities," Water Research Foundation, Report #4408, Denver, CO, 2012.

[9] C. A. Davis, "Water System Service Categories, Post-Earthquake Interaction, and Restoration Strategies," *Earthquake Spectra,* vol. 20, no. 4, pp. 1487-1509, 2014.

[10] L. A. Rossman, "EPANET 2 Users Manual," US Environmental Protection Agency, EPA 600/R–00/057, Cincinnati, OH, 2000.

[11] J. M. Wagner, U. Shamir and D. H. Marks, "Water distribution reliability: Simulation methods," *Journal of Water Resources Planning and Management,* vol. 114, no. 3, pp. 276-294, 1988.

[12] J. Muranho, A. Ferreira, J. Sousa, A. Gomes and A. Sá Marques, "Pressure-dependent demand and leakage modelling with an EPANET extension–WaterNetGen," *Procedia Engineering,* vol. 89, pp. 632-639, 2014.

[13] J. Muranho, A. Ferreira, J. Sousa, A. Gomes and A. Sá Marques, "WaterNetGen - an EPANET extension for automatic water distribution networks models generation and pipe sizing," *Water Science and Technology: Water Supply,* vol. 12, no. 1, pp. 117-123, 2012.

[14] Z. Y. Wu, R. H. Wang, T. M. Walski, S. Y. Yang, D. Bowdler and C. C. Baggett, "Efficient pressure dependent demand model for large water distribution system analysis," in *Proceedings of the 8th Annual Water Distribution System Analysis Symposium 2006*, Cincinnati, Ohio, 2008.

[15] N. Trifunovic, "Pattern Recognition for Reliability Assessment of Water Distribution Networks," PhD Dissertation, Delft University of Technology, Delft, Netherlands, 2012.

[16] A. Pathirana, "EPANET2 Desktop Application for Pressure Driven Demand Modeling," in *Proceedings of the 12th Annual Conference of Water Distribution System Analysis 2010*, Tucson, AZ, 2011.

[17] D. Yoo, D. Jung, D. Kang, J. Kim and K. Lansey, "Seismic Hazard Assessment Model for Urban Water Supply Networks," *Journal of Water Resources Planning and Management,* vol. 142, no. 2, 2016.

[18] D. Laucelli, L. Berardi and O. Giustolisi, "Assessing climate change and asset deterioration impacts on water distribution networks: Demand-driven or pressure-driven network modeling?," *Environmental Modelling and Software,* vol. 37, pp. 206-216, 2012.

[19] US Environmental Protection Agency (USEPA), "Planning for an Emergency Drinking Water Supply," US Environmental Protection Agency, Office of Research and Development, National Homeland Security Research Center, EPA 600/R-11/054, 2011.

[20] A. Mani, M. Tabesh and M. R. Zolfaghari, "Hydraulic performance of post-earthquake water distribution networks based on head driven simulation method," *Water Science and Technology: Water Supply,* vol. 13, no. 5, pp. 1281-1288, 2013.

[21] P. Shi and T. D. O`Rourke, "Seismic Response Modeling of Water Supply Systems," National Center for Earthquake Engineering Research, Technical Report MCEER-08-0016, Buffalo, NY, 2008.

[22] I. Markov, M. Grigoriu and T. O’Rourke, "An Evaluation of Seismic Serviceability of Water Supply Networks With Application to the San Francisco Auxiliary Water Supply System," National Center for Earthquake Engineering Research, Technical Report NCEER-94-0001, Buffalo, NY, 1994.

[23] American Lifelines Alliance (ALA), "Seismic Fragility Formulations for Water Systems, Part 1," American Lifelines Alliance, 2001.

[24] American Lifelines Alliance (ALA), "Seismic Fragility Formulations for Water Systems, Part 2," American Lifelines Alliance, 2001.

[25] American Lifelines Alliance (ALA), "Seismic Guidelines for Water Pipelines," American Lifelines Alliance, 2005.

[26] R. Guidotti, H. Chmielewski, V. Unnikrishnan, P. Gardoni, T. McAllister and J. van de Lindt, "Modeling the resilience of critical infrastructure: the role of network dependencies," *Sustainable and resilient Infrastructure, in press,* 2016.

[27] T. Tabucchi, "Modeling Post-Earthquake Restoration of the Los Angeles Water Supply System," M.S. Thesis submitted to Cornell University, Ithaca, NY, 2007.

[28] N. Romero, "Seismic Hazards and Water Supply Performance," M.S. Thesis submitted to Cornell University, Ithaca, NY, 2009.

[29] X. J. Irias, W. Cain, R. McMullin and Y. Prashar, "Rapid Modeling of Seismic Damage to Water Infrastructure," in *7th U.S. – Japan Workshop on Water System Seismic Practices*, Niigata, Japan, 2011.

[30] D. J. Wald, B. C. Worden, V. Quitoriano and K. L. Pankow, "ShakeMap Manual: Technical Manual, User’s Guide, and Software Guide," United States Geological Survey, Advanced National Seismic System, 2006.

[31] A. A. Hagberg, D. A. Schult and P. J. Swart, "Exploring network structure, dynamics, and function using NetworkX," in *Proceedings of the 7th Python in Science Conference (SciPy2008)*, Pasadena, CA, 2008.

[32] W. McKinney, Python for Data Analysis: Data Wrangling with Pandas, NumPy, and IPython, Sebastopol, CA: O'Reilly Media, 2012.

[33] J. D. Hunter, "Matplotlib: A 2D Graphics Environment," *Computing in Science & Engineering,* vol. 9, pp. 90-95, 2007.

[34] S. van der Walt, S. C. Colbert and G. Varoquaux, "The NumPy Array: A Structure for Efficient Numerical Computation," *Computing in Science & Engineering,* vol. 13, pp. 22-30, 2011.

[35] Python Software Foundation, "Python," 2016. [Online]. Available: https://www.python.org/. [Accessed 2016 6 June].

[36] D. Steffelbauer and D. Fuchs-Hanusch, "OOPNET: An object-oriented EPANET in Python," *Procedia Engineering,* vol. 119, pp. 710-718, 2015.

[37] K. Kawashima, K. Aizawa and K. Takahashi, "Attenuation of peak ground motion and absolute acceleration response spectra," in *Proceedings of the 8th World Conference on Earthquake Engineering (WCEE)*, San Francisco, CA, 1984.

[38] C. E. Baag, S. J. Chang, N. D. Jo and J. S. Shin, "Evaluation of seismic hazard in the southern part of Korea," in *Proceedings of 2nd International Symposium on Seismic Hazards and Ground Motion in the Region of Moderate Seismicity*, 1998.

[39] K. Lee and K. H. Cho, "Attenuation of peak horizontal acceleration in the Sino-Korean Craton," in *Proceedings of the Annual Fall Conference of Earthquake Engineering Society of Korea*, 2002.

[40] Y. X. Yu and C. Y. Jin, "Empirical peak ground velocity attenuation relatioships based on digital broadband records," in *The 14th World Conference on Earthquake Engineering*, Beijing, China, 2008.

[41] R. Isoyama, E. Ishida, K. Yune and T. Shirozu, "Seismic damage estimation procedure for water supply pipelines," in *Proceedings of the 12th World Conference on Earthquake Engineering (WCEE)*, Auckland, New Zealand, 2000.

[42] Federal Emergency Management Agency (FEMA), "Multi-hazard loss estimation methodology, Earthquake model, Hazus-MH 2.1, Technical manual," Washington, DC, 2013.

[43] Federal Emergency Management Agency (FEMA), "Multi-hazard loss estimation methodology, Flood model, Hazus-MH, Technical manual," Washington, DC, 2013.

[44] D. A. Crowl and J. F. Louvar, Chemical Process Safety: Fundamentals with Applications, Upper Saddle River, NJ: Prentice Hall, 2002.

[45] A. Lambert, "What do we know about pressure-leakage relationships in distribution systems," in *IWA Conference: Systems Approach to Leakage Control and Water Distribution Systems Management*, Brno, Czech Republic, 2000.

[46] A. M. Cassa, J. E. van Zyl and R. F. Laubscher, "A numerical investigation into the effect of pressure on holes and cracks in water supply pipes," *Urban Water Journal,* vol. 7, no. 2, pp. 109-120, 2010.

[47] C. T. Kelley, "Solving Nonlinear Equations with Newton's Method," Society for Industrial and Applied Mathematics, Philadelphia, PA, 2003.

[48] K. Barker, J. E. Ramirez-Marquez and C. M. Rocco, "Resilience-based network component importance measures," *Reliability Engineering and System Safety,* vol. 117, pp. 89-97, 2013.

[49] E. Todini, "Looped water distribution networks design using a resilience index," *Urban Water,* pp. 115-122, 2000.

[50] J. P. Watson, R. Murray and W. Hart, "Formulation and optimization of robust sensor placement problems for drinking water contamination warning systems," *Journal of Infrastructure Systems,* vol. 15, no. 4, pp. 330-339, 2009.

[51] International Code Council (ICC), "International Fire Code, Appendix B - Fire-Flow Requirements for Buildings," International Code Council, ISBN: 978-1-60983-046-5, 2012.

Figures

A

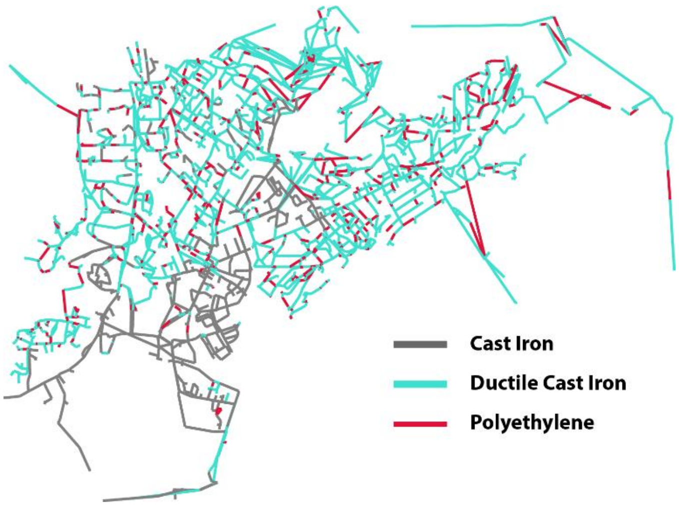

B

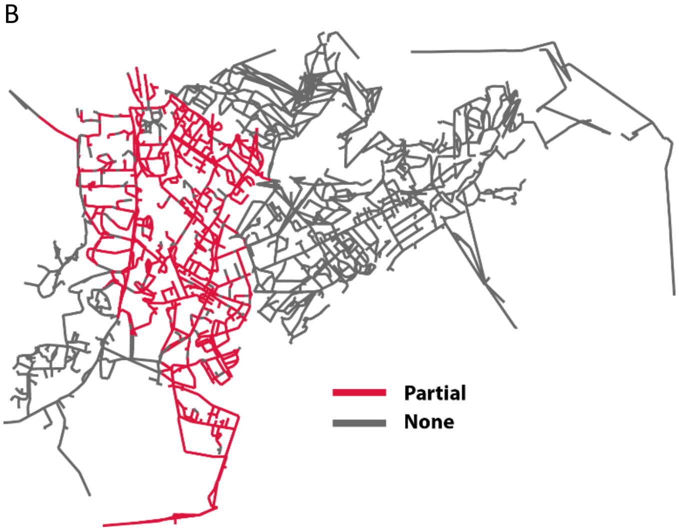

Figure 1. Water distribution network model showing A) pipe material and B) liquefaction potential.

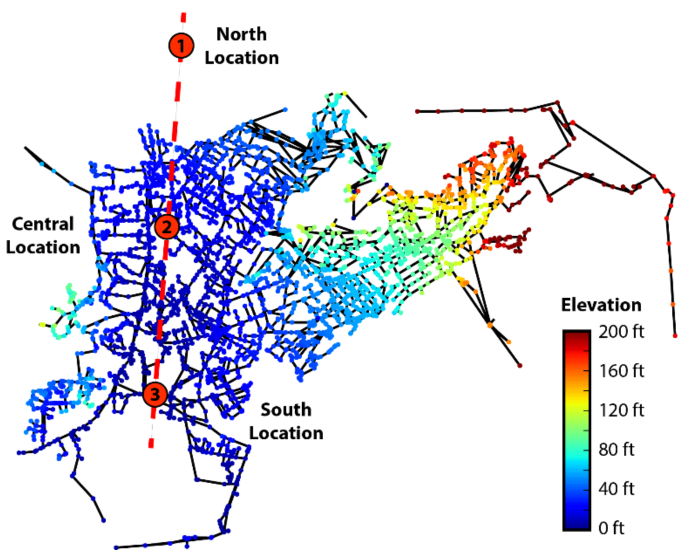

Figure 2. Water distribution network model showing the fault line (dashed red line), node elevation, and epicenter of three earthquakes.

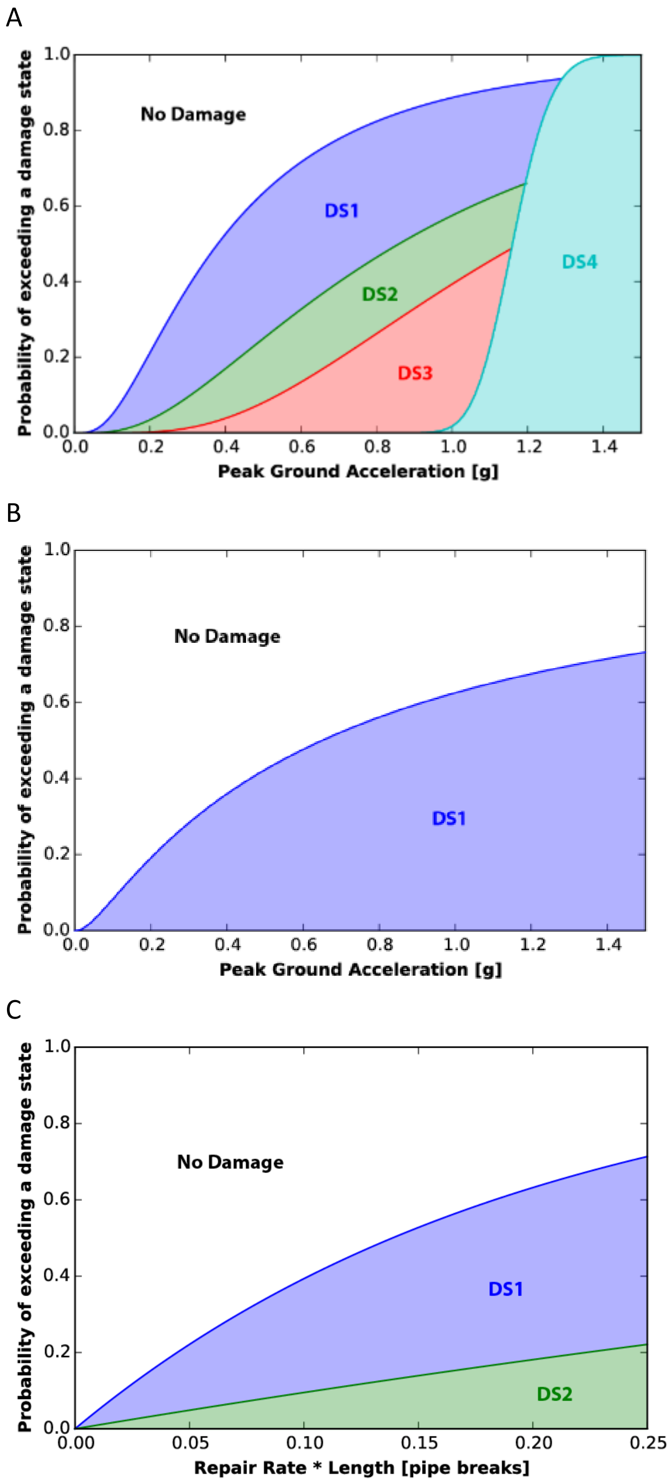

Figure 3. Fragility curves for A) tank, B) pump, and C) pipe damage.

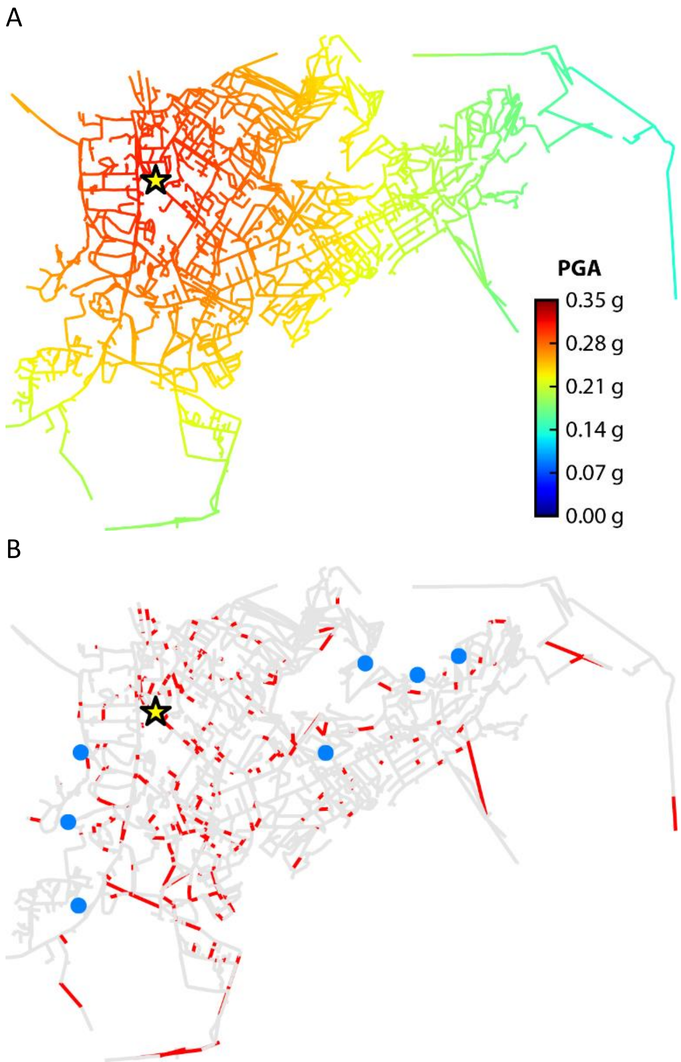

Figure 4. A) PGA and B) location of pipe damage (in red) and tank damage (in blue) for a magnitude of 6.5 earthquake at the central epicenter location. The yellow star indicates the location of the central epicenter.

A

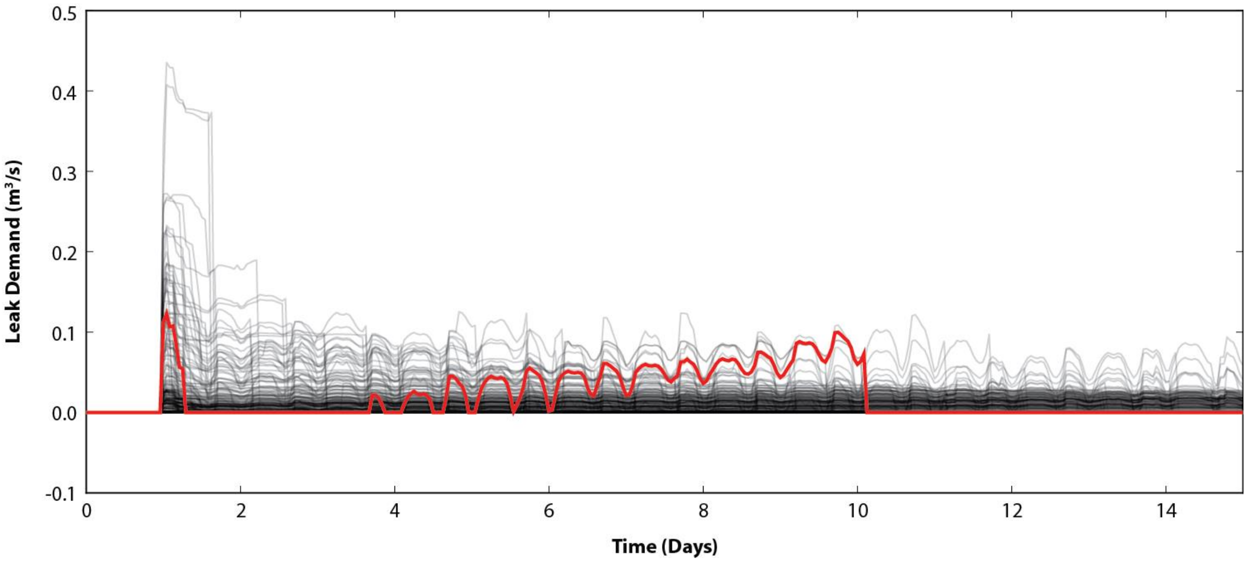

B

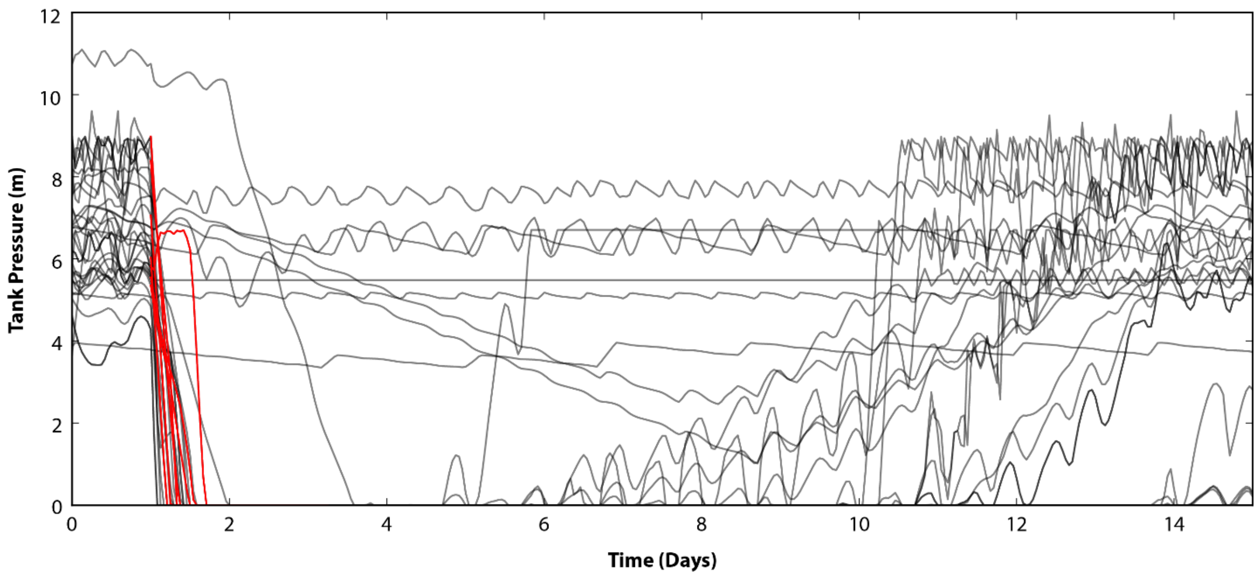

Figure 5. (A) Leak rate and (B) tank level as a function of time for a single realization of a magnitude 6.5 earthquake at the central location using no conservation (RS1). In A), a particular leak is shown in red illustrating the possibility of a leak becoming more prominent as the system is restored. In B) damaged tanks are shown in red up until the time they are repaired, tanks are refilled as the system is restored.

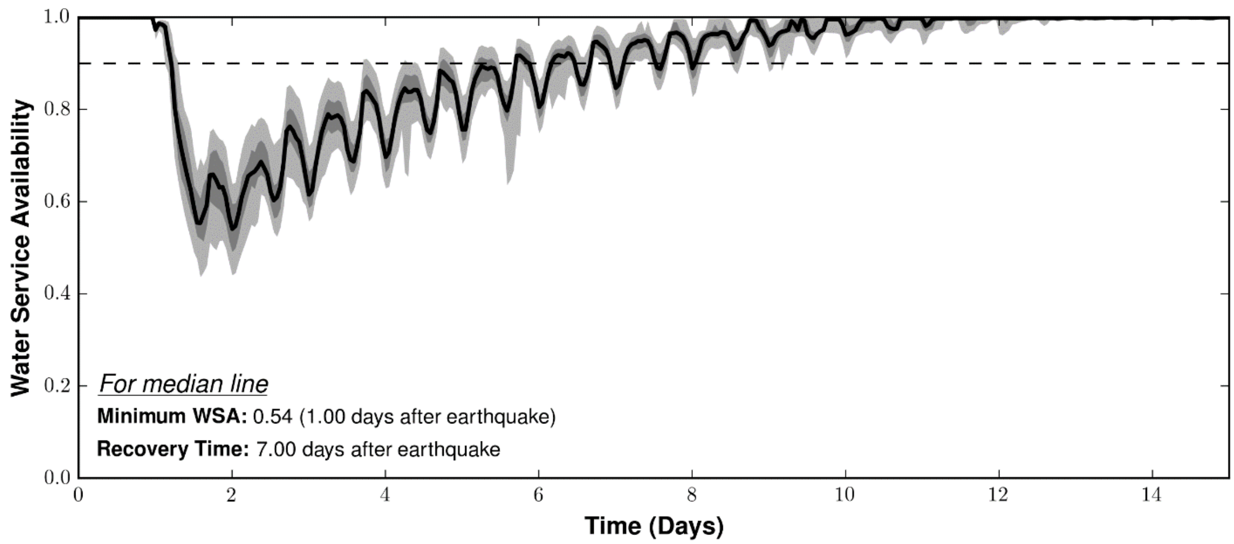

Figure 6. Water service availability for a magnitude 6.5 earthquake at the central location using no conservation (RS1). Light gray is the 5th-95th percentile, dark gray is the 25th-75th percentile, and the black line is the median. Threshold for recovery time shown as a dotted line.

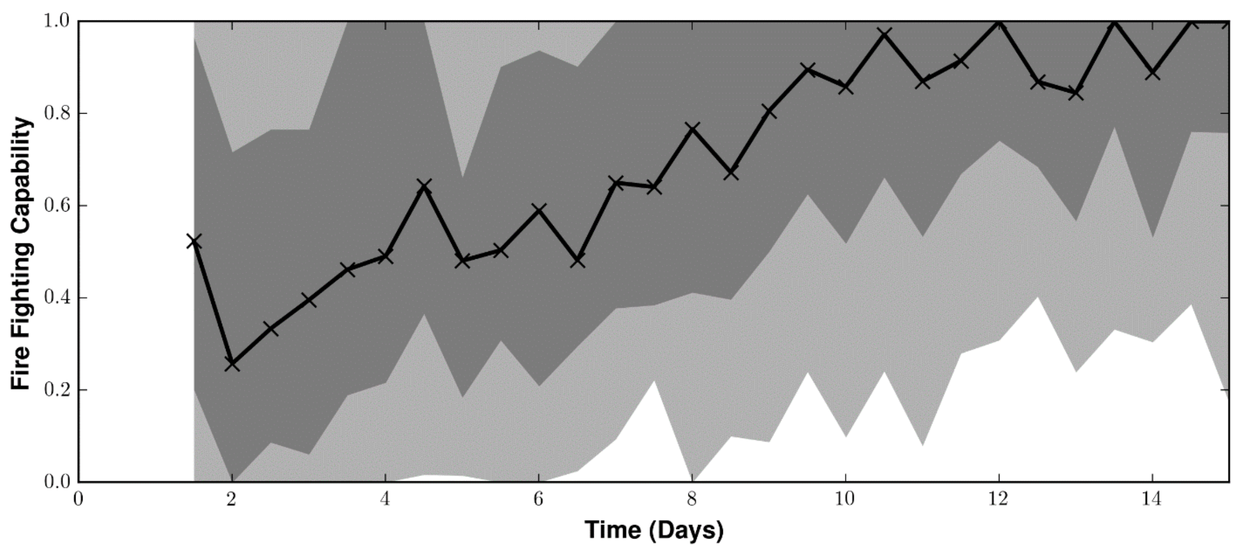

Figure 7. Firefighting capacity for a magnitude 6.5 earthquake at the central location using no conservation (RS1). Light gray is the 5th-95th percentile, dark gray is the 25th-75th percentile, and the black line is the median. Firefighting capacity is computed every 12 hours (indicated by x's) at the location of a particular fire.

A

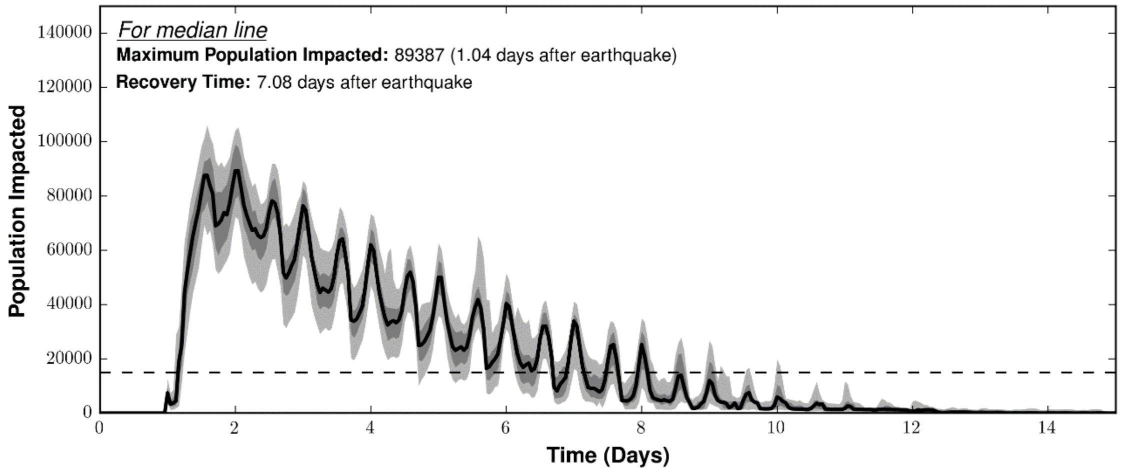

B

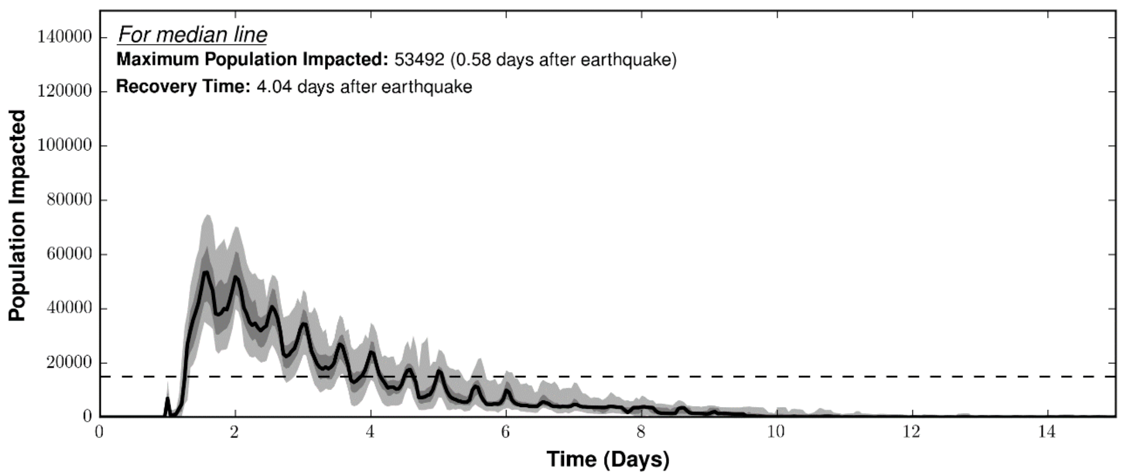

C

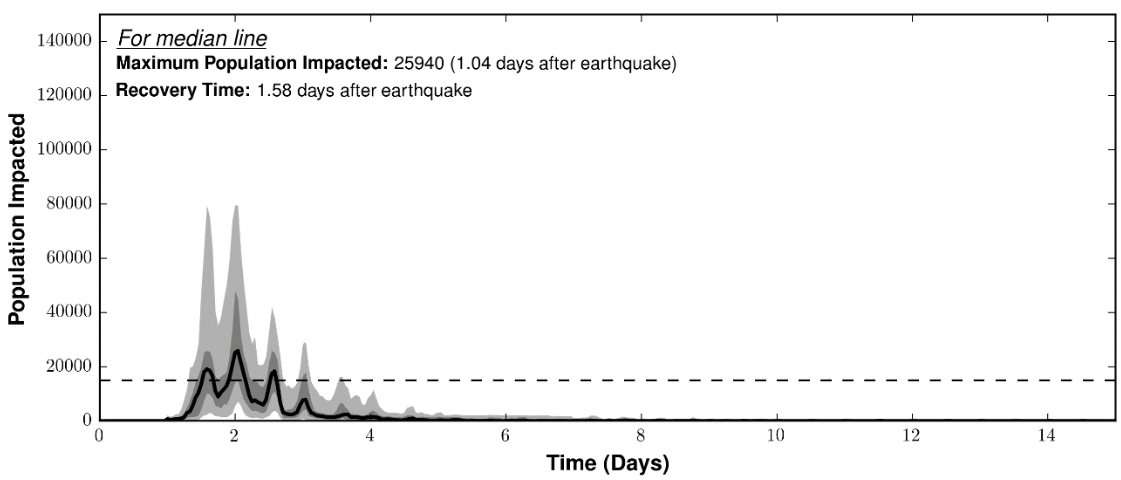

Figure 8. Population impacted (A) without conservation (RS1), (B) with conservation (RS2), and (C) with seismic-resistant pipes (RS3) for 50 realizations of a magnitude 6.5 earthquake at the central location. Light gray is the 5th-95th percentile, dark gray is the 25th-75th percentile, and the black line is the median. Threshold for recovery time shown as a dotted line.

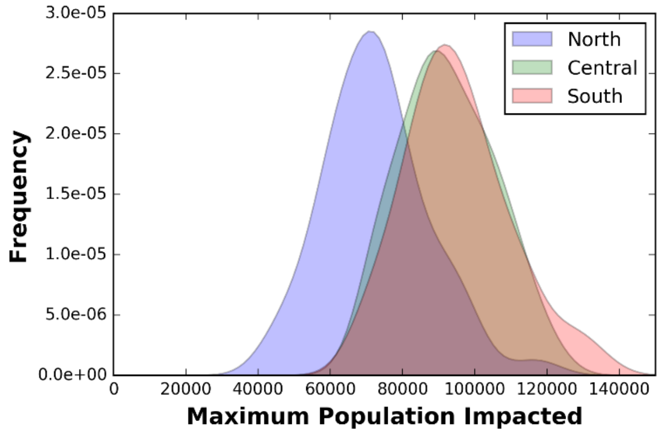

Figure 9. Effect of location of the earthquake on maximum population impacted for a 6.5 magnitude earthquake at the central location and no conservation (RS1).

Tables

Table 1. Minimum water service availability (WSA) and recovery time for each earthquake magnitude, location, and repair strategy. Values are computed using the median of the 50 realizations. A recovery time of 0 means that the median value never went below 90% water service availability.

		South Location		*Central Location*		*North Location*	
Repair Strategy	**Magnitude**	**Minimum WSA**	**Recovery Time in Days**	**Minimum WSA**	**Recovery Time in Days**	**Minimum WSA**	**Recovery Time in Days**
RS1 (Pipe, tank, pump repair & firefighting)	**6.0**	0.88	1.04	0.85	1.08	0.98	0.00
	6.5	0.53	6.04	0.54	7.00	0.65	4.04
	7.0	0.28	14.00+	0.27	14.00+	0.35	14.00+
RS2 (RS1 with 40% water conservation)	**6.0**	0.98	0.00	0.97	0.00	1.00	0.00
	6.5	0.66	3.08	0.67	4.00	0.79	1.58
	7.0	0.37	14.00+	0.35	14.00+	0.45	9.04
RS3 (RS1 with seismic-resistant pipes)	**6.0**	1.00	0.00	1.00	0.00	1.00	0.00
	6.5	0.83	1.08	0.87	1.08	0.93	0.00
	7.0	0.45	6.04	0.50	6.04	0.60	4.04

Table 2. Maximum population impacted and recovery time for each earthquake magnitude, location, and repair strategy. Values are computed using the median of the 50 realizations. A recovery time of 0 means that the median value never went above 10% population impacted.

		South Location		*Central Location*		*North Location*	
Repair Strategy	**Magnitude**	**Max Pop. Impacted**	**Recovery Time in Days**	**Max Pop. Impacted**	**Recovery Time in Days**	**Max Pop. Impacted**	**Recovery Time in Days**
RS1 (Pipe, tank, pump repair & firefighting)	**6.0**	27142	1.08	33902	1.58	2548	0.00
	6.5	90736	7.00	89387	7.08	71520	4.58
	7.0	127398	14.00+	129232	14.00+	118908	14.00+
RS2 (RS1 with 40% water conservation)	**6.0**	4378	0.00	4260	0.00	302	0.00
	6.5	57167	3.58	53492	4.04	32260	2.00
	7.0	104194	14.00+	105814	14.00+	89560	10.00
RS3 (RS1 with seismic-resistant pipes)	**6.0**	551	0.00	1060	0.00	646	0.00
	6.5	36984	1.58	25940	1.58	13971	0.00
	7.0	104518	6.04	93146	7.04	73782	4.08